Light-Responsive Polyelectrolyte/Gold Nanoparticle Microcapsules

Alexandra S. Angelatos, Benno Radt, and Frank Caruso*

Center for Nanoscience and Nanotechnology, Department of Chemical and Biomolecular Engineering, The University of Melbourne, Parkville, Victoria 3010, Australia

Received: October 28, 2004; In Final Form: December 3, 2004

We report the preparation and characterization of light-responsive delivery vehicles, microcapsules composed of multiple polyelectrolyte layers and light-absorbing gold nanoparticles. The nanostructured capsules were loaded with macromolecules (fluorescein isothiocyanate-labeled dextran) by exploiting the pH-dependence of the shell permeability, and the encapsulated material was released on demand upon irradiation with short (10 ns) laser pulses in the near-infrared (1064 nm). In addition, the polyelectrolyte multilayer shell was modified with lipids (dilauroylphosphatidylethanolamine) and then functionalized with ligands (monoclonal immunoglobulin G antibodies) for the purposes of enhanced stability and targeted delivery, respectively. We anticipate that these capsules will find application in a range of areas where controlled delivery is desirable.

1. Introduction

Stimuli-responsive delivery vehicles have, over the years, attracted significant interest for applications in the areas of medicine, pharmaceutics, agriculture, and the food and cosmetics industries. Key requirements of the delivery vehicles in, for example, bioapplications are: (i) that they can be controllably loaded with active materials; (ii) that they are stable during storage and circulation; (iii) that they transport their load specifically to the targeted site; and (iv) that they release their load in a controlled manner. A number of stimuli-responsive delivery vehicles have been proposed. Typically, the active material is immobilized on or entrapped within liposomes or polymeric particles and undergoes release in response to an environmental trigger such as a change in pH, temperature, ionic strength, and/or enzyme concentration.[1] However, recent efforts have focused on the development of optically addressable delivery systems,[2,3] because irradiation with light promises to be an effective means of releasing the active material. For example, the advent of phototriggerable liposomes[2a] has permitted control over the release rate from liposomal drug delivery vehicles. Mal and co-workers[2b] have prepared mesoporous silica with coumarin derivatives attached to the pore outlets that allow the release of guest molecules following irradiation with ultraviolet (UV) light. Ipe et al.[2c] have designed a photoswitchable double-shell structure comprising a gold nanoparticle core with photochromic spiropyran molecules anchored to the surface, forming the first shell. The spiropyran molecules regulate the assembly and release of an outer shell of amino acid derivatives upon irradiation with UV light and visible light, respectively. Sershen and co-workers[2d] have developed a photothermally responsive macroscopic hydrogel (i.e., a copolymer of *N*-isopropylacrylamide and acrylamide incorporating gold−gold sulfide nanoshells), which undergoes a dramatic volume collapse upon illumination with light in the near-infrared (NIR), a region where most tissues show only weak light absorption.[4] Laser-induced release of dye and protein molecules entrapped within the composite material was demonstrated;[2d] however, the system has not as yet been translated to colloidal delivery vehicles. Recently, Tao et al.[2e] reported polyelectrolyte/congo red capsules that become increasingly permeable on exposure to visible light, and Skirtach and co-workers[2f] reported polyelectrolyte/silver nanoparticle capsules that exhibit a maximum absorption at ca. 430 nm. However, the release of biologically significant materials from these capsules was not investigated. To this end, we recently reported the fabrication of optically addressable nanostructured capsules comprising a polyelectrolyte multilayer shell doped with light-absorbing gold nanoparticles.[3] It was shown that the enzyme lysozyme can be encapsulated within the polyelectrolyte/gold nanoparticle shell via layer-by-layer (LbL) assembly on the surface of lysozyme crystals and that the enzyme can be released on demand without significant loss of bioactivity following irradiation with short pulses of NIR laser light.

Herein, we report the loading/release of macromolecules into/from light-responsive polyelectrolyte/gold nanoparticle microcapsules, as well as the modification and biofunctionalization of the polyelectrolyte multilayer shell with lipids and ligands, respectively (Scheme 1). In contrast to our previous study where the enzyme was used as a template to achieve encapsulation, here fluorescein isothiocyanate (FITC)-labeled dextran, a convenient model of high molecular weight biomaterials such as DNA, was post-loaded into preformed capsules by switching the capsule permeability between the "closed" and "open" states through variation of the bulk solution pH.[5] Fluorescence spectroscopy revealed that the FITC-dextran was released from the capsules upon irradiation with 10 ns laser pulses at 1064 nm, provided the capsules contained gold nanoparticles within their shell. Electron microscopy confirmed that the laser irradiation had no apparent effect on capsules without the light-absorbing shell component. In addition, the polyelectrolyte multilayer shell was coated with dilauroylphosphatidylethanolamine (DLPE)[6] for enhanced stability and subsequently functionalized with monoclonal immunoglobulin G (IgG) antibodies for targeted delivery. The homogeneity of the lipid coating and the ligand coverage was verified via fluorescence microscopy, while the ability of the lipid coating to restrict the passage of molecules across the polyelectrolyte multilayer shell was demonstrated by UV−visible spectroscopy.

* Corresponding author. E-mail: fcaruso@unimelb.edu.au.

10.1021/jp045070x CCC: $30.25
Published on Web 01/26/2005

SCHEME 1: Schematic Illustration of the Various Colloidal Systems Investigated[a]

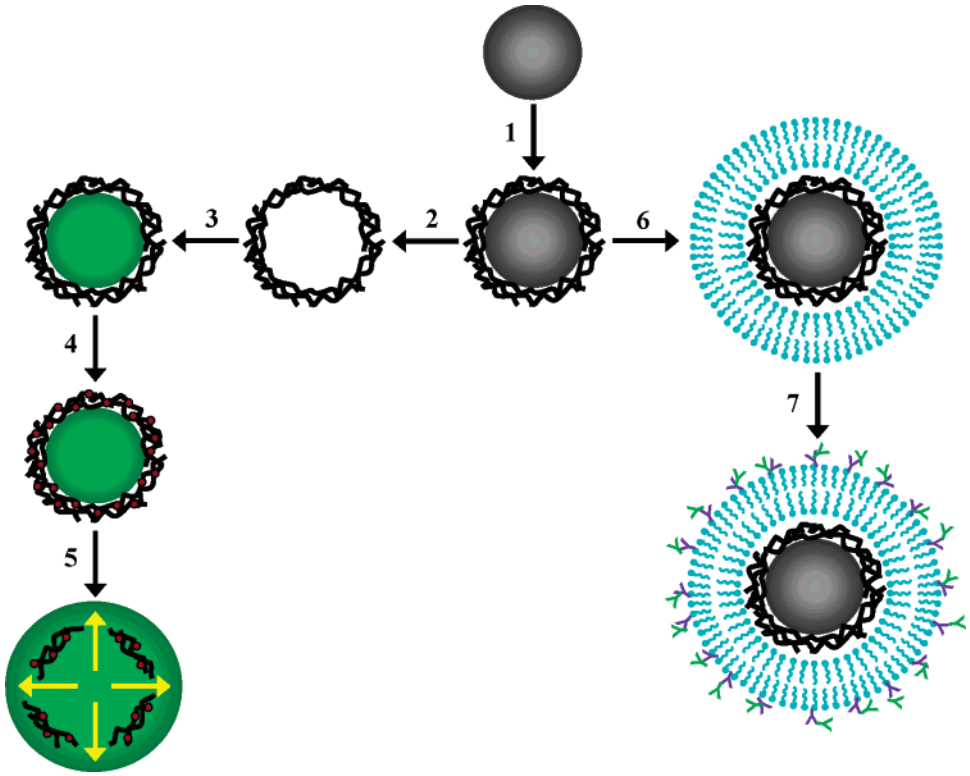

[a] (1) LbL coating of colloidal templates with polyelectrolytes to yield core−shell particles; (2) decomposition of the colloidal templates to yield polyelectrolyte multilayer capsules; (3) loading of macromolecules into the capsules by exploiting the pH-dependence of the shell permeability; (4) infiltration of light-absorbing gold nanoparticles into the capsule shell to render the capsules optically addressable; (5) release of the encapsulated material on demand using short pulses of NIR laser light; (6) modification of the polyelectrolyte multilayer shell with lipids; and (7) biofunctionalization of the polyelectrolyte multilayer shell with a primary anitbody and subsequent binding of a fluorescently-labeled secondary antibody.

2. Experimental Section

2.1. Materials. All materials were purchased from Sigma-Aldrich and used as received except for the acid-decomposable melamine formaldehyde (MF) particles, which were obtained from Microparticles GmbH. The water employed was prepared in a three-stage Millipore Milli-Q Plus 185 purification system (resistivity > 18.2 MΩ cm).

2.2. Preparation of the Capsules. MF particles (diameter 1.39 ± 0.06 μm, concentration 0.4 wt. %) were incubated in an aqueous poly(sodium 4-styrenesulfonate) (PSS) solution (average PSS M_w 70 000, PSS concentration 1 mg mL^{-1}, sodium chloride (NaCl) concentration 0.5 M, pH 7) for 20 min with continual stirring. This was followed by three cycles of centrifugation (1000*g*, 3 min)/supernatant exchange (with water)/redispersion. Poly(allylamine hydrochloride) (PAH) (average M_w 70 000) was subsequently adsorbed from solution (PAH concentration 1 mg mL^{-1}, NaCl concentration 0.5 M, pH 7) using the same procedure. The entire process was repeated a further three times to produce core−shell particles comprising MF particles coated with four PSS/PAH bilayers (i.e., eight polyelectrolyte layers). To decompose the MF templates, the core−shell particles were exposed to hydrochloric acid (HCl) (final HCl concentration 0.1 M) for 20 min with continual stirring. This was followed by three cycles of centrifugation (5000*g*, 5 min)/supernatant exchange (with water)/redispersion, yielding a suspension of PSS/PAH multilayer capsules. Note that the outermost layer of the core−shell particles was PAH (positive) prior to HCl addition to minimize the adsorption of positively charged MF decomposition products from solution onto the outer shell surface during the core decomposition process.[7] To produce capsules with a negative outer surface charge and hence reduce the adherence of capsules to the Eppendorf tube wall, a ninth polyelectrolyte layer (PSS) was then adsorbed.

2.3. Loading of FITC-Dextran into the Capsules. Dextran (average M_w 10 500), labeled with 0.01 mol of FITC per mol of glucose, was added to the capsules in phosphate buffered saline (PBS) at pH 5 (final FITC-dextran concentration 1 mg mL^{-1}), and the mixture was stirred for 3 h. FITC-dextran in Tris buffer at pH 9 was then added (final FITC-dextran concentration 1.1 mg mL^{-1}), and the mixture was stirred for 30 min. This was followed by three cycles of centrifugation (1000*g*, 5 min)/supernatant exchange (with Tris buffer)/redispersion.

2.4. Release of FITC-Dextran from the Capsules. Prior to the laser experiments, gold nanoparticles (average diameter 6 nm) were infiltrated into the shell of the capsules loaded with FITC-dextran by incubating the capsules for 3 h with continual stirring in a solution of the gold nanoparticles stabilized by 4-(dimethylamino)pyridine (DMAP).[8] This was followed by three cycles of centrifugation (800*g*, 5 min)/supernatant exchange (with Tris buffer)/redispersion. An additional polyelectrolyte layer (PSS) was then adsorbed to produce capsules with a negative outer surface charge and hence reduce the adherence of capsules to the Eppendorf tube wall. The laser experiments involved irradiating dispersions of the capsules loaded with FITC-dextran, with and without the light-absorbing gold nanoparticles in their shell, in a 3 mL quartz cuvette equipped with a magnetic stirrer bar. Irradiation was at 1064 nm for 5 min with a 10 Hz series of 10 ns pulses (radiant exposure per pulse 700 mJ cm^{-2}) from a Q-switched neodymium:yttrium-aluminum-garnet (Nd:YAG) laser beam (diameter ca. 5 mm). The Nd:YAG NY-61 laser (Continuum Inc., USA) was operated at a

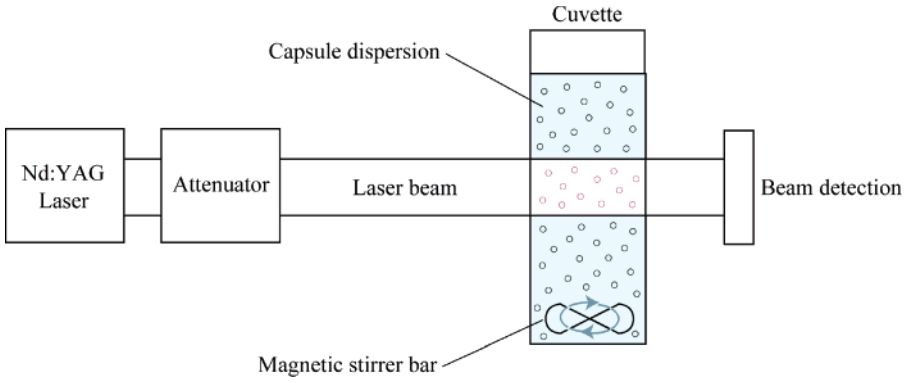

Figure 1. Setup employed in the laser experiments.

high pump power (400 mJ per pulse output) to achieve a homogeneous top hat multimode laser profile and was attenuated to the lower energies required using an adjustable polarizing beam splitter to keep the beam profile constant in all experiments. The setup employed in the laser experiments is illustrated in Figure 1. Immediately following the laser experiments, the irradiated capsule dispersions and the equivalent nonirradiated capsule dispersions were centrifuged (800*g*, 5 min), and then FITC-dextran fluorescence emission spectra were recorded for the supernatants recovered. In each case, the excitation wavelength was set at 490 nm (i.e., the fluorescence excitation maximum of FITC-dextran).

2.5. Modification of the Polyelectrolyte Multilayer Shell. DLPE in ethanol was added to the MF core−PSS/PAH shell particles (final DLPE concentration 1 mM), and the mixture was stirred for 30 min. This was followed by three cycles of centrifugation (8000*g*, 10 min)/supernatant exchange (with water)/redispersion. To observe the lipid coating under the fluorescence microscope, (i) 1,6-diphenyl-1,3,5-hexatriene (DPH) was added to the lipid-coated core−shell particles (final DPH concentration 0.1 μM), and (ii) FITC was covalently coupled to the lipid coating by incubating the lipid-coated core−shell particles in FITC (final FITC concentration 0.1 mg mL^{-1}) for 45 min with continual stirring, followed by three cycles of centrifugation (300*g*, 5 min)/supernatant exchange (with water)/redispersion. As a control experiment, core−shell particles fabricated from PSS and poly(diallyldimethylammonium chloride) (PDADMAC) (average M_w 150 000) were similarly coated with DLPE and then studied via fluorescence microscopy. The surface of the core−shell particles rather than that of the capsules was modified with lipids (and subsequently functionalized with antibodies) so that the permeability of the lipid assembly could be readily examined through decomposition of the core; that is, HCl was added to the MF core−PSS/PAH shell particles with and without the DLPE coating (final HCl concentration 1 mM), after which a series of extinction spectra were recorded.

2.6. Biofunctionalization of the Polyelectrolyte Multilayer Shell. Monoclonal IgG antibodies were attached to the surface of the lipid-coated MF core−PSS/PAH shell particles via electrostatic association; that is, the particles were incubated with continual stirring in (i) purified mouse IgG (final primary antibody concentration 0.1 mg mL^{-1}) for 3 h, (ii) bovine serum albumin (BSA) (final BSA concentration 0.1 mg mL^{-1}) for 20 min, and then (iii) FITC-labeled rabbit anti-mouse IgG (final secondary antibody concentration 0.1 mg mL^{-1}) for 30 min. Each of these adsorption steps was performed at pH 7 and followed by three cycles of centrifugation (1000*g*, 3 min)/supernatant exchange (with PBS)/redispersion. As a control experiment, the lipid-coated core−shell particles were incubated in BSA and the secondary antibody, but not the primary antibody.

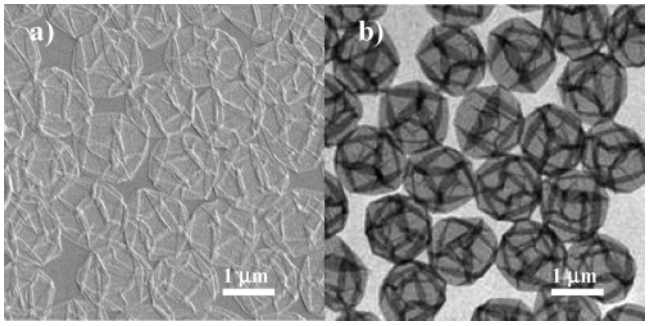

Figure 2. (a) SEM and (b) TEM images of PSS/PAH capsules.

2.7. Characterization. Samples were examined/imaged using an Olympus BHS fluorescence microscope, a Philips XL30 FEG field emission scanning electron microscope (SEM) operated at 2 kV, and a Philips CM120 BioTWIN transmission electron microscope (TEM) operated at 120 kV. Fluorescence and extinction spectra were recorded using a Varian Cary Eclipse fluorescence spectrometer and an Agilent 8453 UV−visible spectrophotometer, respectively.

2.8. General. All experiments were performed at room temperature, and all samples were stored under refrigeration. Samples involving FITC or DPH were prepared and stored in opaque Eppendorf tubes.

3. Results and Discussion

3.1. Preparation of the Capsules. Polyelectrolyte multilayer capsules were prepared by applying the LbL technique[9] to colloidal templates.[10] This involved the sequential deposition of PSS and PAH from solution onto weakly cross-linked MF resin[11] microparticles, exploiting electrostatic interactions for multilayer build-up. The templating MF cores were subsequently decomposed with HCl to yield PSS/PAH multilayer microcapsules (Figure 2). Micrometer-sized templates were selected to facilitate microscopic observation of the capsules, while the PSS/PAH polyelectrolyte pair was chosen as it is one of the most widely used for producing multilayer films on both planar and colloidal surfaces.

3.2. Loading of FITC-Dextran into the Capsules. Under most conditions, polyelectrolyte multilayer capsules assembled on MF templates are readily permeable to small molecules such as ions and dyes. The permeability of such capsules to macromolecules is, however, considerably more selective. It can be reversibly switched from the "closed" to the "open" state by varying the bulk solution properties (e.g., pH, ionic strength,

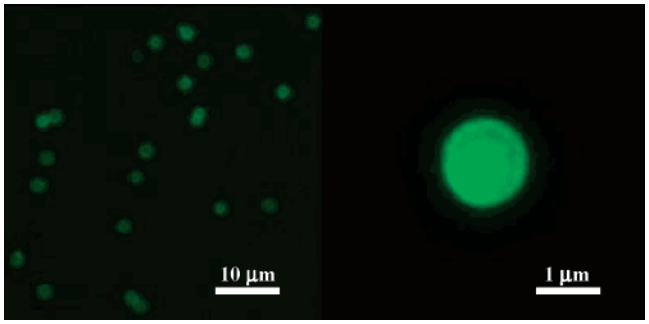

Figure 3. Fluorescence microscope images of PSS/PAH capsules loaded with FITC-dextran. The fluorescence observed originates from the FITC label on the dextran molecules within the capsules.

temperature), thereby allowing the capsules to be loaded with macromolecules.[5,7,12]

In this work, FITC-dextran (i.e., a polymer of anhydroglucose with FITC randomly conjugated to the free hydroxyl groups) was employed as the probe macromolecule because it is a convenient model of high molecular weight biomaterials such as DNA. The PSS/PAH multilayer capsules were loaded with FITC-dextran (Figure 3) by exploiting the pH-dependence of the shell permeability. This involved lowering the pH to 5 ("open" state) to induce permeation of FITC-dextran into the capsules, and then increasing the pH to 9 ("closed" state) to entrap the molecules that had diffused into the capsules so that the excess FITC-dextran could be removed from the bulk solution.[5]

The increased permeability of the capsules upon lowering the pH below the value at which they were assembled may be attributed to charging of the weak polyelectrolyte component, PAH. This leads to swelling (i.e., loosening of the polyelectrolyte multilayers) and pore formation. Factors such as mechanical stress during the core decomposition, retention of MF oligomers within the polyelectrolyte network, and adsorption of the probe macromolecule to the capsule walls may also influence the permeability of the capsules.[5]

3.3. Release of FITC-Dextran from the Capsules. The PSS/PAH multilayer capsules loaded with FITC-dextran were rendered optically addressable by infiltrating gold nanoparticles into the polyelectrolyte network.[8] The use of gold nanoparticles as the light-absorbing component offers a number of advantages. First, relative to the absorption of individual gold nanoparticles, the absorption of gold nanoparticles within the capsule shell is red-shifted to the NIR region (700−1500 nm),[3] where most tissues show only weak light absorption.[4] Second, the extent of the red-shift can be tuned by varying the number of gold nanoparticle layers within the capsule shell.[3] Third, because the pulses of NIR laser light used to induce release are short, the laser light energy is effectively confined to the capsule shell and so encapsulated biomaterials undergo negligible activity loss upon release.[3] Fourth, the absorption of gold nanoparticles within the capsule shell is broad relative to the absorption of individual gold nanoparticles, and thus a number of different laser sources may be employed to address the capsules.[3]

Release of FITC-dextran was achieved by irradiating the polyelectrolyte/gold nanoparticle capsules at 1064 nm with a series of 10 ns pulses (radiant exposure per pulse 700 mJ cm^{-2}) from a Q-switched Nd:YAG laser. Capsules loaded with FITC-dextran but without light-absorbing gold nanoparticles in their shell were similarly irradiated as a control experiment. Immediately following the laser irradiation, the capsule dispersions were centrifuged and then FITC-dextran fluorescence emission spectra were recorded for the supernatants recovered. For the

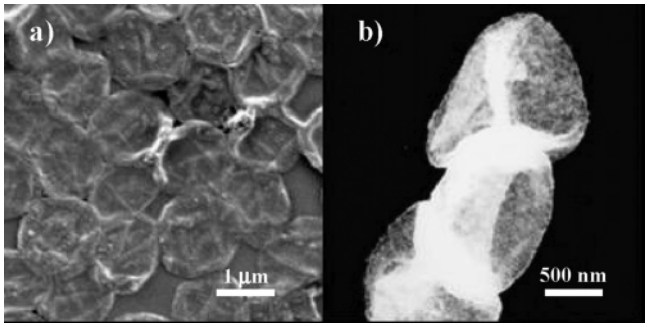

Figure 4. (a) SEM and (b) TEM images of PSS/PAH/gold nanoparticle capsules loaded with FITC-dextran before laser irradiation.

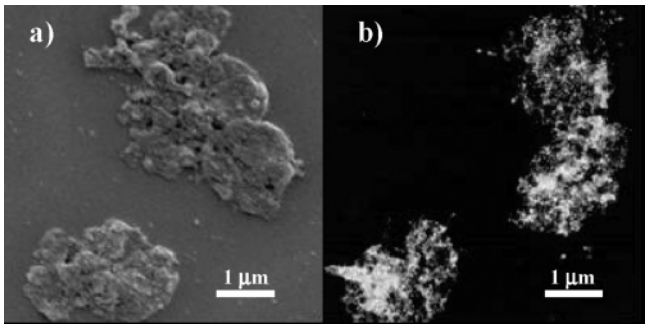

Figure 5. (a) SEM and (b) TEM images of PSS/PAH/gold nanoparticle capsules loaded with FITC-dextran after laser irradiation (radiant exposure per pulse 700 mJ cm^{-2}).

polyelectrolyte/gold nanoparticle capsules loaded with FITC-dextran, laser irradiation produced a significant increase (ca. 850%) in the supernatant fluorescence at 520 nm (i.e., the fluorescence emission maximum of FITC-dextran). However, for the capsules loaded with FITC-dextran but without gold nanoparticles in their shell, the increase in the supernatant fluorescence at 520 nm upon laser irradiation was negligible. This shows that the short NIR laser pulses induced release of FITC-dextran from the polyelectrolyte/gold nanoparticle capsules, whereas the capsules without the light-absorbing shell component were unaffected (with respect to macromolecule permeability) by the high radiant exposures (700 mJ cm^{-2}) employed.

The effects of the laser irradiation were further investigated using electron microscopy. Figures 4 and 5 show electron microscope images of the FITC-dextran-loaded polyelectrolyte/gold nanoparticle capsules before and after laser exposure, respectively. Prior to laser irradiation, the dried capsules resembled deflated balloons (Figure 4a), and there was a homogeneous dense packing of gold nanoparticles (which appear bright in TEM) within the capsule shells (Figure 4b). After laser irradiation, however, the outlines of individual capsules could no longer be readily discerned (Figure 5a), and there was evidence of gold nanoparticle fusion among the remnants of the capsules (Figure 5b). Importantly, the FITC-dextran-loaded capsules without gold nanoparticles in their shell closely resembled the capsules shown in Figure 2, both before and after laser irradiation. This confirms that the high radiant exposures employed had no apparent effect on the morphology of the capsules without the light-absorbing gold nanoparticles in their shell.

Our findings, in conjunction with the findings of previous optical studies,[13] suggest that a plausible mechanism for the laser-induced release involves: (i) the heating of the capsule shell to temperatures in excess of the spinodal point of water and the melting point of gold (600−800 °C)[14] due to the gold

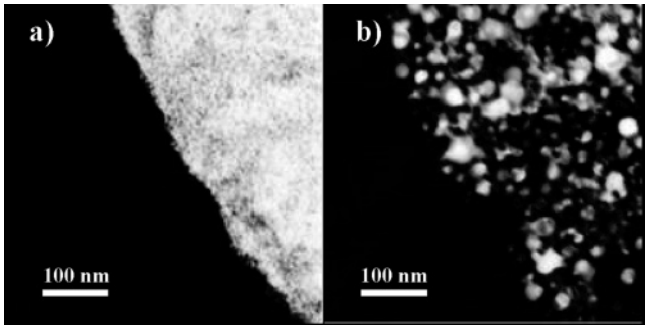

Figure 6. TEM images of a section of a PSS/PAH/gold nanoparticle capsule loaded with FITC-dextran (a) before and (b) after laser irradiation (radiant exposure per pulse 700 mJ cm^{-2}).

nanoparticles within the polyelectrolyte multilayers absorbing the laser light energy; (ii) the development of significant thermal stresses within the capsule shell because its various components have different thermal expansion coefficients; and (iii) the ultimate rupture of the capsule shell. Figure 6 shows high magnification TEM images of a typical FITC-dextran-loaded polyelectrolyte/gold nanoparticle capsule before laser exposure (Figure 6a) and after laser exposure (Figure 6b). Figure 6a illustrates the initial homogeneous dense packing of the gold nanoparticles (average diameter 6 nm) within the capsule shell, while Figure 6b provides evidence that the capsule shell is heated to temperatures in excess of the melting point of gold during the laser-induced release, as it clearly shows the melting/fusion of the gold nanoparticles upon laser irradiation. The size distribution of the gold nanoparticles among the remnants of the irradiated capsules is relatively broad, with diameters ranging from ca. 6 nm to ca. 45 nm. Other phenomena that may also play a role in the laser-induced release include: (i) phase explosions[4] around the gold nanoparticles, that is, the transformation of the surrounding superheated (metastable) water to an equilibrium state of mixed phase via spinodal decomposition, which involves the rapid spontaneous growth of small density fluctuations that extend over large spatial scales; and (ii) electron ejection[15] from the gold nanoparticles, that is, the partial conversion of the gold nanoparticles into ions which diffuse away and are later chemically reduced to form new smaller gold nanoparticles.

3.4. Modification of the Polyelectrolyte Multilayer Shell. Assembly of a lipid coating on the outer capsule surface following loading could prevent leakage of the encapsulated material from the capsules prior to release. To investigate this, MF core−PSS/PAH shell particles were coated with the zwitterionic phospholipid DLPE via adsorption of lipid molecules from a saturated ethanol solution.[6] The surface of the core−shell particles rather than that of the capsules was modified with lipids (and subsequently functionalized with antibodies) so that the permeability of the lipid assembly could be readily examined through decomposition of the core (see later). Addition of DPH (i.e., a compound that fluoresces at ca. 430 nm in the presence of lipids) to the particles verified that they were coated with DLPE (Figure 7a and b). The subsequent covalent coupling of FITC to the lipid assembly revealed that the DLPE coating was homogeneous (Figure 7c). Importantly, these experiments were repeated using core−shell particles fabricated from PSS (i.e., the same polyanion) and PDADMAC (i.e., a different polycation that, unlike PAH, lacks the functionality required to couple to FITC). The fluorescence microscope images obtained in this case were indistinguishable from those shown in Figure 7. This indicates that the uniform fluorescence from the particles in Figure 7c arose from the coupling of FITC to the lipid assembly rather than the coupling of FITC to the PAH molecules within the shell and hence confirms that the DLPE coating on the MF core−PSS/PAH shell particles was homogeneous.

To determine whether the lipid assembly impeded the passage of molecules across the polyelectrolyte multilayer shell, MF core−PSS/PAH shell particles with and without the DLPE coating were exposed to 1 mM HCl, after which a series of extinction spectra were recorded for each sample to monitor the MF core decomposition process. Figure 8 shows the MF core extinction at 265 nm as a function of time after HCl addition for core−shell particles with (○) and without (●) the DLPE coating. In the case of the core−shell particles without the DLPE coating, the extinction dropped instantly upon acid addition and then decayed linearly for the remainder of the experiment. In the case of the core−shell particles with the DLPE coating, however, the extinction was effectively constant over the duration of the experiment. These results suggest that, while diffusion of HCl ions from the bulk solution through the shell to the MF core occurrs in both cases[10b], diffusion of the resulting MF decomposition products through the shell into the bulk solution only occurred in the case of the core−shell particles without the DLPE coating. The fact that the lipid assembly completely restricted the passage of MF decomposition products through the shell into the bulk solution provides further evidence that the DLPE coating on the MF core−PSS/PAH shell particles was homogeneous.

3.5. Biofunctionalization of the Polyelectrolyte Multilayer Shell. One approach to achieve targeted delivery is through the use of ligands such as antibodies, peptides, polysaccharides, and aptamers.[16] In this work, monoclonal IgG antibodies were attached to the surface of the MF core−PSS/PAH shell particles

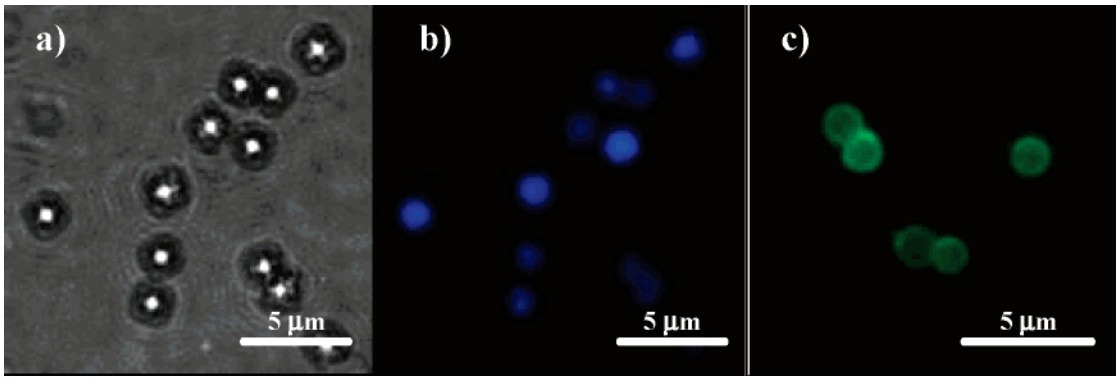

Figure 7. Fluorescence microscope images of MF core−PSS/PAH shell particles coated with DLPE: (a) particles illuminated by transmitted light; (b) the same particles in (a) illuminated by a mercury lamp to reveal the DPH fluorescence; and (c) particles with FITC covalently coupled to the lipid coating.

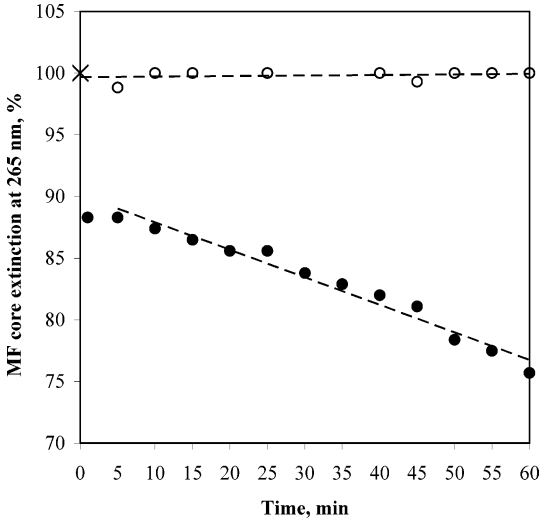

Figure 8. Variation in the MF core extinction at 265 nm (expressed as a percentage of the initial MF core extinction at 265 nm) with time after addition of 1 mM HCl to MF core−PSS/PAH shell particles with (○) and without (●) a DLPE coating. The initial data point (0 min, 100%), denoted by a cross, applies to both systems.

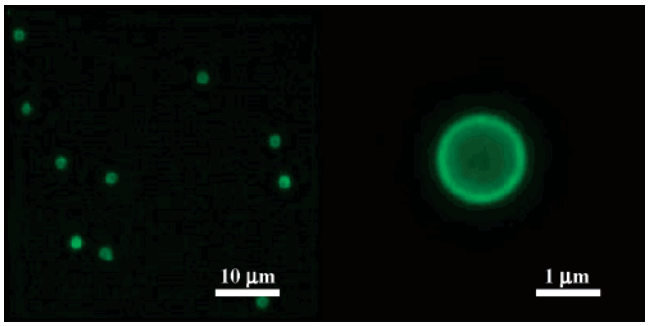

Figure 9. Fluorescence microscope images of MF core−PSS/PAH shell particles coated with DLPE and functionalized with antibodies, mouse IgG (primary antibody) and FITC-labeled rabbit anti-mouse IgG (secondary antibody). The fluorescence observed originates from the FITC label on the secondary antibody.

coated with DLPE via electrostatic association. First, a primary antibody (mouse IgG) was coupled to the lipid coating to impart biospecificity. After incubating the particles with BSA to block any potential nonspecific binding sites, the particles were then exposed to a FITC-labeled secondary antibody (rabbit anti-mouse IgG) to probe the nature of the lipid coating/primary antibody coupling. Each of these three adsorption steps was performed at pH 7. Fluorescence microscopy revealed a homogeneous surface coverage of the FITC-labeled secondary antibody, and hence the primary antibody (Figure 9). As a control experiment, DLPE-coated core−shell particles were incubated with BSA followed by the FITC-labeled secondary antibody (i.e., the primary antibody coupling step was omitted). The fluorescence observed in this case was negligible. This indicates that the fluorescence in Figure 9 arose from the coupling of the FITC-labeled secondary antibody to the primary antibody and hence confirms that the primary antibody was homogeneously attached to the DLPE coating.

4. Conclusions

Light-responsive microcapsules, comprising PSS/PAH multilayers infiltrated with gold nanoparticles, were prepared via the LbL colloid-templating technique. It was shown that FITC-dextran can be loaded into the capsules by exploiting the pH-dependence of the shell permeability, and then released on demand from the capsules by irradiating with 10 ns pulses of laser light at 1064 nm. Capsules without light-absorbing gold nanoparticles in their shell were unaffected by such laser irradiation. Hence, the laser-induced release is attributed to gold nanoparticle-mediated heating of the capsule shell, which ultimately causes it to rupture. It was also shown that the polyelectrolyte multilayer shell can be (i) modified with a homogeneous DLPE coating, which restricts the passage of molecules across the shell and so could serve to prevent leakage from the capsules in the period between loading and release, and (ii) functionalized with monoclonal IgG antibodies, which could facilitate delivery of the capsules specifically to a targeted site. The capsules presented herein have the potential to impact a broad range of disciplines as their properties may be readily tailored to specific applications by simply varying the shell composition (e.g., the inclusion of biocompatible/biodegradable materials[7,17] may render the capsules suitable for in vivo delivery).

Acknowledgment. We gratefully acknowledge the financial support of the Australian Research Council (Discovery Project and Federation Fellow schemes) and the Alexander von Humboldt Foundation. We thank Ken Ghiggino and Trevor Smith, Simon Crawford, and Elisabeth Hill for use of the laser, microscopic, and spectroscopic equipment, respectively. We also thank Kiyofumi Katagiri, John Quinn, Yajun Wang, and Felix Meiser for contributing their materials and/or valuable expertise.

References and Notes

(1) Yang, L.; Alexandridis, P. *Curr. Opin. Colloid Interface Sci.* **2000**, *5*, 132.

(2) (a) Shum, P.; Kim, J.-M.; Thompson, D. H. *Adv. Drug Delivery Rev.* **2001**, *53*, 273. (b) Mal, N. K.; Fujiwara, M.; Tanaka, Y. *Nature* **2003**, *421*, 350. (c) Ipe, B. I.; Mahima, S.; Thomas, K. G. *J. Am. Chem. Soc.* **2003**, *125*, 7174. (d) Sershen, S.; Westcott, S. L.; Halas, N. J.; West, J. L. *J. Biomed. Mater. Res.* **2000**, *51*, 293. (e) Tao, X.; Li, J.; Möhwald, H. *Chem.-Eur. J.* **2004**, *10*, 3397. (f) Skirtach, A. G.; Antipov, A. A.; Shchukin, D. G.; Sukhorukov, G. B. *Langmuir* **2004**, *20*, 6988.

(3) Radt, B.; Smith, T. A.; Caruso, F. *Adv. Mater.* **2004**, *16*, 2184.

(4) Vogel, A.; Venugopalan, V. *Chem. Rev.* **2003**, *103*, 577.

(5) Antipov, A. A.; Sukhorukov, G. B.; Leporatti, S.; Radtchenko, I. L.; Donath, E.; Möhwald, H. *Colloids Surf., A* **2002**, *198−200*, 535.

(6) Moya, S.; Donath, E.; Sukhorukov, G. B.; Auch, M.; Bäumler, H.; Lichtenfeld, H.; Möhwald, H. *Macromolecules* **2000**, *33*, 4538.

(7) Khopade, A. J.; Caruso, F. *Chem. Mater.* **2004**, *16*, 2107.

(8) Gittins, D. I.; Susha, A. S.; Schoeler, B.; Caruso, F. *Adv. Mater.* **2002**, *14*, 508.

(9) Decher, G.; Hong, J.-D. *Ber. Bunsen-Ges. Phys. Chem.* **1991**, *95*, 1430.

(10) (a) Caruso, F.; Caruso, R. A.; Möhwald, H. *Science* **1998**, *282*, 1111. (b) Donath, E.; Sukhorukov, G. B.; Caruso, F.; Davis, S. A.; Möhwald, H. *Angew. Chem., Int. Ed.* **1998**, *37*, 2201. (c) Caruso, F. *Adv. Mater.* **2001**, *13*, 11. (d) Caruso, F. *Aust. J. Chem.* **2001**, *54*, 349. (e) Caruso, F., Ed. *Colloids and Colloid Assemblies: Synthesis, Modification, Organization and Utilization of Colloidal Particles*; Wiley-VCH: Weinheim, 2003.

(11) Angelatos, A. S.; Burgar, M. I.; Dunlop, N.; Separovic, F. *J. Appl. Polym. Sci.* **2004**, *91*, 3504.

(12) (a) Sukhorukov, G. B.; Brumen, M.; Donath, E.; Möhwald, H. *J. Phys. Chem. B* **1999**, *103*, 6434. (b) Ibarz, G.; Dähne, L.; Donath, E.; Möhwald, H. *Adv. Mater.* **2001**, *13*, 1324.

(13) (a) Kamat, P. V. *J. Phys. Chem. B* **2002**, *106*, 7729. (b) Pitsillides, C. M.; Joe, E. K.; Wei, X.; Anderson, R. R.; Lin, C. P. *Biophys. J.* **2003**, *84*, 4023. (c) Aguirre, C. M.; Moran, C. E.; Young, J. F.; Halas, N. J. *J. Phys. Chem. B* **2004**, *108*, 7040.

(14) Buffat, P.; Borel, J. P. *Phys. Rev. A* **1976**, *13*, 2287.

(15) McGrath, T. E.; Beveridge, A. C.; Diebold, G. J. *Angew. Chem., Int. Ed.* **1999**, *38*, 3353.

(16) Vyas, S. P.; Singh, A.; Sihorkar, V. *Crit. Rev. Ther. Drug Carrier Syst.* **2001**, *18*, 1.

(17) Schüler, C.; Caruso, F. *Biomacromolecules* **2001**, *2*, 921.